Received: 23 April 2020 | Revised: 18 December 2020 | Accepted: 20 December 2020

DOI: 10.1111/fog.12527

ORIGINAL ARTICLE

FISHERIES OCEANOGRAPHY WILEY

# Characterising Essential Fish Habitat using spatio-temporal analysis of fishery data: A case study of the European seabass spawning areas

Chloé Dambrine | Mathieu Woillez | Martin Huret | Hélène de Pontual

Ifremer, Plouzané, France

**Correspondence**
Chloé Dambrine, Ifremer, STH, F29280 Plouzané, France.
Email: chloe.dambrine@orange.fr

**Funding information**
Institut Français de Recherche pour l'Exploitation de la Mer; France Filière Pêche; European Maritime and Fisheries Fund, Grant/Award Number: 400017DM0720006; Ministère de l'Agriculture et de l'Alimentation

## Abstract

Fish habitats sustain essential functions for fish to complete their life cycle, such as feeding, growing and spawning. Conservation is crucial to maintain fish populations and their exploitation. Since 2013, the spawning stock biomass of the northern stock of European seabass (*Dicentrarchus labrax*) has been in a worrying state. A series of low recruitments with a persistently high level of fishing has been blamed, raising concerns about the processes involved in seabass reproduction and settlement in nurseries. Here, we characterise seabass spawning areas along the French Atlantic coast using vessel monitoring system (VMS) data. A non-linear geostatistical approach was applied, from 2008 to 2014, to detect locations where seabass aggregate for spawning. Occurrence maps of spawning distribution were combined into probability maps to quantify the seasonal and inter-annual variability and to highlight recurrent, occasional and unfavourable spawning areas. We identified three main spawning areas: the Rochebonne Plateau in the Bay of Biscay, the Western English Channel and the North of the Cotentin peninsula in the Eastern English Channel. The correlative link between this geographical distribution and environmental factors was investigated using a Bayesian spatio-temporal model. The spatio-temporal structure accounted for the vast majority of the model predictive skills, whereas environmental covariates had a negligible effect. Our model revealed the persistence of the spatial distribution of spawning areas with intra- and inter-annual variability. Offshore areas appear to be essential spawning areas for seabass, and should be considered in spatial management strategies.

**KEYWORDS**
Bay of Biscay, Bayesian spatio-temporal modelling, *Dicentrarchus labrax*, english Channel, European sea bass, non-linear geostatistics, spawning grounds

## 1 | INTRODUCTION

Fish live in different habitats depending on their life stages (Harden Jones, 1968). Finding the right environmental conditions (e.g. temperature, food and oxygenation) is critical for them to achieve the phases of their life cycle and maximise the vital functions involved (e.g. growth and reproduction). These environments have been listed as 'Essential Fish Habitats' in the Magnuson-Stevens Fishery Act (2007) as follows: 'those waters and substrate necessary to fish for spawning, breeding, feeding or growth to maturity'. Spawning areas,

nurseries, migrations paths (active and passive) and feeding areas are considered essential because the successful renewal of the population relies on their good state. Spawning and nursery areas are characterised by a high concentration of individuals in a restricted area (Dahlgren et al., 2006; Domeier, 2012). It is therefore crucial to understand and describe their spatial and temporal variations to prevent overfishing in these areas when the population is vulnerable.

Following a series of poor recruitments associated with high fishing pressure (ICES, 2012), the spawning stock biomass of European seabass (*Dicentrarchus labrax*) in the North Atlantic is worrying. It raises concerns about our understanding of the habitats of this species. De Pontual et al. (2019) confirmed the fidelity of the species to feeding areas, and show evidence of fidelity behaviour to spawning areas. In the North Atlantic, information about European seabass spawning areas is very scarce, and no scientific survey has ever assessed seabass spawning aggregations (e.g. adult or egg sampling). The only data available are from the fisheries. However, several biases have been listed (Maunder et al., 2006) that are related to fishermen's knowledge and intention (targeting or not), gear selectivity, resource catchability and external conditions (e.g. weather conditions, fuel price and management measures). Besides, these data do not follow a consistent sampling plan, and it is challenging to correlate catches to species abundance in a given area. Thus, it is important to account for these biases when using fishery data to avoid wrong conclusions.

The methods for detecting large fish aggregation or spots of overabundance (hotspots), such as those found in spawning areas, have been reviewed by Nelson and Boots (2008). Most of the time, hotspots are defined after one has applied a species distribution model on catches or densities (e.g. Colloca et al., 2009) or, less frequently, using raw data (e.g. densities from scientific survey; Petitgas et al., 2016). Moreover, according to these authors, in ecology, hotspots are often detected using an arbitrary density or catch threshold above which a species is considered to aggregate. This method was used by Large et al. (2009) to study where blue ling aggregate to reproduce. Since then, attempts have been made to decrease the subjectivity of the threshold approach, while trying to take into account the neighbourhood of the observation. Bartolino et al. (2011) used the analysis of the tangent to the cumulative relative frequency distribution (CRFD) curve, whereas Petitgas et al. (2016) developed a geostatistical modelling approach. The originality of the geostatistical approach is that it uses spatial structural tools (variogram, cross-variogram), which allow the definition and modelling of the spatial extent of the hotspots with minimal subjectivity. A comparison between these two methods (Petitgas et al., 2016) showed that the hotspots highlighted using the geostatistical method are larger and colder, but better defined thanks to the tools used.

The spatial distribution of fish is not random and depends on external (e.g. the environment) and internal (e.g. density-dependence processes) population controls (Planque et al., 2011). Species distribution modelling, which is of growing interest in fishery ecology (e.g. Bellido et al., 2008; Brodie et al., 2015), must, therefore, take this into account. Traditionally, generalised linear or additive models (GLM/GAM) are used to relate the presence or abundance of a species to environmental variables. However, using these models assumes that the observations are independent, which is often not the case in fishery data (Kneib et al., 2008). This spatial correlation, therefore, needs to be considered to avoid wrong conclusions. A Bayesian hierarchical spatial or spatio-temporal approach is an suitable tool to account for this spatial dependency. Such approaches are of growing importance in fishery science (e.g. Munoz et al., 2013; Paradinas et al., 2015). Compared to frequentist methods, they allow using probability to represent the uncertainty in the inputs and outputs of the model. It is also possible to attribute a random effect to the spatial component. The use of such methods has been simplified by the development of the integrated nested Laplace approximation (INLA; Rue et al., 2009) and its associated R package (Rue et al., 2014).

In this paper, our objective was to characterise the spawning areas of the European seabass in the Bay of Biscay–English Channel area. We applied the geostatistical approach of Petitgas et al. (2016) to a fishery dataset over the period 2008–2014. Studying their seasonal and inter-annual variability, we highlight the most contributing spawning areas. We, then, tested environmental covariates using an INLA geostatistical modelling approach to explain the spatio-temporal distribution of these spawning areas over the whole study area during the spawning season.

## 2 | MATERIAL AND METHODS

### 2.1 | Characterisation of the spawning areas

#### 2.1.1 | Data description

Our fishery data represented catches for all vessels that caught seabass at least once a year in the English Channel–Celtic Sea–Bay of Biscay area. The spatial extent of the fishery data is illustrated in Figure 1. On average, 74.5% of the study area was covered by observations each month. The lack of data was mainly due to the ban on fishing along the coast.

Data were extracted from the French SACROIS flow (Demanèche et al., 2010) for the period 2008–2014. Recent years were not considered since a series of management measures were set since 2015 in the Celtic Sea–English Channel area, and one of them ban pelagic trawling, method known to fish on spawning areas (ICES, 2018). SACROIS is a cross-validation tool that is similar to the approach developed by Hintzen et al. (2012). It assembles data from different declarative sources including the French fleet register, annual surveys of fishing activity calendars, logbooks (vessels >10 m) and monthly declarative forms (vessels <10 m), sales and geolocation data (VMS). By comparing the consistency between these information, SACROIS provides the best available data for each fishing trip.

From this flow, we gathered a table containing estimated production data (e.g. quantity of a species broken down in commercial

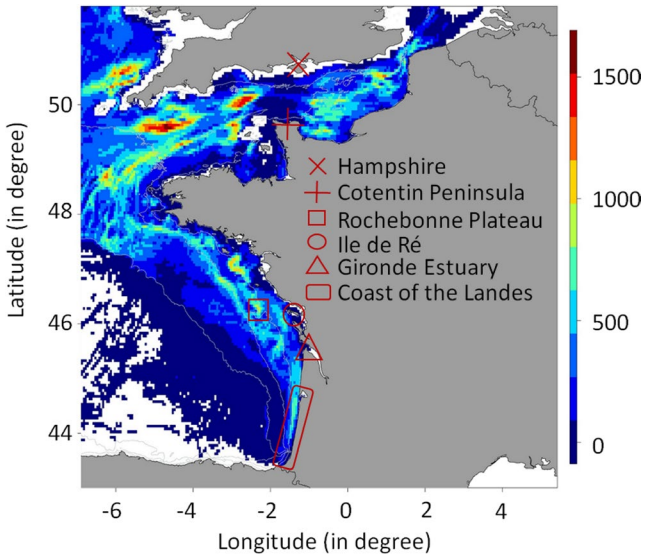


**FIGURE 1** The study area and the spatial extent of the fishery data focused on the Bay of Biscay and the English Channel. Grid cells are coloured depending on their yearly average number of fishing hauls. Grey lines represent the isobaths 100, 200 and 300 m. Red symbols highlight locations of interest [Colour figure can be viewed at wileyonlinelibrary.com]

categories (kg) and duration of the fishing operations (h)) per week, per square of three nautical miles and per fishing vessel. We summed the data to obtain a fishing duration and a quantity of seabass per month and square. When seabass were absent from the fishing sets, the amount was set to 0 kg. Since a minimum conservation reference size (MCRS; close to the size of the species at maturity) is applied to seabass catches, and only adult fish migrate to spawning areas (juveniles remain in coastal nurseries), it can be assumed that the proportion of juveniles in the catches was negligible, at least during the spawning period.

Using fisheries data implies having information only where fishermen have prospected. To maintain the broadest spatial coverage in our study, we focused on the gears that presented the highest seabass catch rates on average during the whole year or that targeted seabass in winter. The analysis was restricted to midwater otter (OTM) and pair trawls (PTM), bottom otter (OTB) and pair trawls (PTB), otter twin trawls (OTT), set gillnets (GNS), trammel nets (GTR), purse seines (PS) and Danish seines (SDN). On average, each square of three nautical miles was fished eight times each month. The yearly gear composition and the fishery spatial distribution over the studied period can be found in (Figures S1, S2 and S3). The considered fishery remained more or less stable in space and time. The gear composition varies over space (i.e. depending on the location, different gears are dominant). However, the gear composition map is rather stable over time, meaning that we do not expect temporal changes in fishing efficiency and therefore catch per unit effort (CPUE) estimates. The main gears are OTB, OTT and PTM. They account on average for 43.4%, 28.5% and 8.3%, respectively, with PTM presenting the highest average catch rates for seabass (23 kg.h$^{-1}$).

For our analysis, we considered CPUE data (kg.h$^{-1}$) averaged over gears by squares and months. This variable makes it possible to capture the core of the distribution of the seabass spawning areas, even though some biases exist and will be discussed hereafter. For instance, some small spawning areas may be unnoticed because they are not fished or they are exploited by a gear with a lower fishing efficiency than those producing the highest catch rates.

### 2.1.2 | Non-linear geostatistical approach

To detect the seabass spawning areas, we used the hotspots analysis developed by Petitgas et al. (2016). As we had no or limited information on the seabass spawning period, we described hotspots for each month of the years in the studied time series. We also split the study area, because the average of CPUE data differed between the two main ICES management units: the English Channel–Celtic Sea stock (i.e. latitudes ≥ N 48°) and the Bay of Biscay stock (i.e. latitudes < N 48°) and because the value of the highest cut-off depends on the global mean (Petitgas et al., 2016).

First, the CPUE variable was coded into indicator functions using ten cut-off values: 0.5, 1, 5, 10, 20, 50, 100, 200, 500 and 1000 kg.h$^{-1}$ of seabass/month/square. For instance, the indicator (i.e. presence/absence) of the geometrical set $A_i$ defined for the cut-off $z_i$ is:

$$1_{A_i}(x) = \begin{cases} 1 \text{ if } Z(x) \geq z_i \\ 0 \text{ if } Z(x) < z_i \end{cases}$$

with $Z(x)$ in the the CPUE value square $x$. A geometrical set is defined as a collection of distinct objects, in our case CPUE values, for which we have examined how they are shaped or organised in space.

Three geostatistical structural tools, based on these indicators, were used: (i) the simple variogram $\gamma_i(h)$ of the geometrical set $A_i$, which measures the probability of entering into $A_i$ for various distance vectors $h$; (ii) the ratio of the cross-variogram of the geometrical sets $A_{i+1}$ and $A_i$ (with $z_{i+1} > z_i$) on the simple variogram of $A_i$, $\frac{\gamma_{i\times(i+1)}(h)}{\gamma_i(h)}$, which quantifies the transition probability of getting inside $A_{i+1}$ when entering into $A_i$ from distance $h$, and (iii) the variogram of the residuals of the regression between $1_{A_{i+1}}(x)$ and $1_{A_i}(x)$, which quantifies the spatial behaviour within $A_i$ of the values higher than $z_{i+1}$.

Then, we searched the geometrical set $A_i$ that represents the hotspots of the spatial distribution of the CPUE values. To do so, we computed the structural tools for the different cut-offs, and then searched the highest cut-off $z_i$, which fulfils the following four criteria: (i) the variogram $\gamma_i(h)$ is structured (i.e. increases for the first distance lags and then flattens (I on Figure 2); (ii) the variogram $\gamma_{i+1}(h)$ is unstructured (II on Figure 2); (iii) no edge effect is found with the highest geometrical set (III on Figure 2); and (iv) the residuals are possibly unstructured (IV on Figure 2). However, because of the high data sampling density (i.e. series of gridded maps of CPUE values with a resolution of 3 x 3 nmi), the interpretation of the variograms was sometimes difficult.

If the four criteria were not met together, a flat variogram ratio (IV on Figure 2) was considered as the minimal condition to determine which geometrical set should be regarded as a hotspot.

When finding the cut-off $z_i$ for each month of the seven years (2008–2014) in the two areas, we made monthly comparison of the level of the $A_i$ sets that characterise the seabass spawning season. The hypothesis was that higher cut-offs should be found in winter, attesting for the aggregation of seabass to spawn. To check this hypothesis and to confirm the seabass spawning period, we used the gonado-somatic index of seabass in the English Channel (Pawson & Pickett, 1996) and in the Bay of Biscay (ICES, 2018) to keep only months corresponding to the spawning period for each region. For the months of the spawning period, hotspots of the seabass CPUE spatial distribution were considered as seabass spawning areas.

Monthly average maps of seabass spawning areas were produced for each month of the seabass spawning period. To produce those maps, we averaged the value of $1_{A_i}(x)$ between years for each square of a month. The values of $1_{A_i}(x)$ equal to 1 outside the previously defined spawning season were set to 0 to represent fish aggregations for other purposes than reproduction. Our maps thus represent the spawning areas of importance and their variability across years. Spawning areas were classified into three categories depending on the $1_{A_i}(x)$ values in each square, namely: recurring (>0.66), occasionally favourable (0.33–0.66) and unfavourable (<0.33) areas.

## 2.2 | Environmental drivers of the spawning areas distribution

### 2.2.1 | Tested covariates

After characterising seabass spawning areas over the time series, we quantitatively investigated this distribution against environmental covariates. The choice of the covariates was driven by their potential effect on this demersal fish, which has a marked pelagic behaviour, especially during winter-time (de Pontual et al., 2019; Heerah et al., 2017; Woillez et al., 2016). Seabass migrate from coastal areas to offshore areas to spawn (Pawson et al., 2007) and one of the main drivers of this migration is temperature (Pickett & Pawson, 1994). We thus considered temperature as well as salinity and bathymetry as covariates pertinent to illustrate a coast to offshore gradient. The qualitative knowledge of seabass spawning areas distribution seems to correspond to very dynamic oceanographic areas. We thus tested current velocities and surface above geoid (as an indicator of eddy activity). We also considered the physical habitat that characterises the global environment of the fish and tested the ocean mixed layer thickness and the chlorophyll-*a* as general descriptors of the environment for eggs and larvae.

Among the covariates tested, two did not vary over time: the bathymetry (SHOM, 2015) and the EUNIS habitats (Hamdi et al., 2010). The EUNIS habitats were simplified in seven or four habitat classes (Tables S1 and S2). The four habitat classes were based on sediment grain size, while the seven habitat classes were also based on the position in the marine vertical zonation and the exposure to currents and swell. We also considered five physical covariates extracted from the Atlantic—European North West Shelf—Ocean Physics Reanalysis (monthly means): temperature (surface, bottom and mean over the entire water column), salinity (surface and mean over the entire water column), current velocity (surface and mean over the entire water column), ocean mixed layer thickness and surface height above the geoid. The last was a biological covariate: chlorophyll-*a* (monthly mean from satellite observations (daily average) Reprocessed L4 (ESA-CCI)).

We considered two covariates as 'not correlated' if their Pearson correlation coefficient was under 0.7.

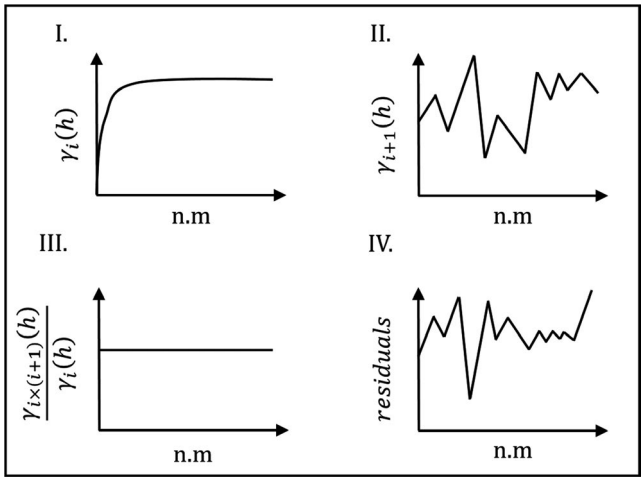


**FIGURE 2** Theoretical situation for which the cut-off $z_i$ of the geometrical set $A_i$ defines a hotspot: (a) the variogram $\gamma_i(h)$ is structured (i.e. shows an increase for the first distance lags and then flattens), (b) the variogram $\gamma_{i+1}(h)$ is unstructured, (c) the variogram ratio $\frac{\gamma_{i\times(i+1)}(h)}{\gamma_i(h)}$ is flat (i.e. $A_{i+1}$ is positioned randomly within $A_i$) and (d) the variogram of the residuals of the regression between $1_{A_{i+1}}(x)$ and $1_{A_i}(x)$ is unstructured

### 2.2.2 | Model approach

To explore the link between the distribution of seabass occurrences and its environment, we implemented a Bayesian hierarchical spatio-temporal model for each area. To reduce the amount of data involved in the computation, we focused our modelling on the months for which spawning events occurred.

To develop the model, we used the integrated nested Laplace approximation (INLA; Rue et al., 2009) approach available in the R-INLA package of the R Statistical Programming software (Rue et al., 2014). This approach captures the spatial dependency using Gaussian Random Fields (GRF; e.g. Bakka et al., 2018). In statistical modelling, a GRF is fully defined by its mean and covariance. The covariance matrix of a GRF can be constructed based on observation location, but too many observations require a considerable computational cost. Lindgren et al. (2011) developed the stochastic

partial differential equation (SPDE) approach to reduce these costs. Instead of building a discrete model for the GRF, this approach constructs a continuous indexed approximation of the GRF with a continuous model of Matérn covariance structure: the SPDE. Computational time is saved because the covariance matrix is not directly computed but deduced from the sparse precision matrix produced with the SPDE. In the R-INLA package (Rue et al., 2014), a mesh (i.e. a triangulation of the study area, which is the best compromise between low computational costs and reasonable accuracy of the GRF representation) is used to approximate the SPDE.

### 2.2.3 | Model development

The developed spatio-temporal model is a combination of linear predictors to explain the observed data (i.e. presence/absence of spawning areas):

$$y_{ijk} \sim \text{Bin}\left(\pi_{ijk}\right)$$

$$g^{-1}\left(\pi_{ijk}\right) = \beta_0 + \beta_{1:n} x_{ijk} + u_{ijk}$$

with $y_{ij}$ the presence or absence of spawning areas at the location $i$ during the month $j$ of the year $k$, $\pi_{ijk}$ the probability of presence, $g$ the logit link function, $\beta_0$ the intercept, $\beta_{1:n}$ the linear effects of the covariates $x_{ijk}$, and $u_{ijk}$ different structures of spatio-temporal random effects. We used an independent zero-mean Gaussian prior for the intercept and the other linear predictors. The spatial component has two parameters $\tau$ and $\kappa$, which correspond to the total variance and the spatial range, respectively. For them, an independent Gaussian prior was used for the reparametrised $\log(\tau)$ and $2\log(\kappa)$.

We first focused on the spatio-temporal structure within the spawning season without considering the inter-annual variability. We tested five different spatio-temporal structures for $u_{ij}$ among those reviewed by Martínez-Minaya et al. (2018). In the first case:

$$u_{ij} = w_{ij}$$

with $w_{ij}$ x spatial realisations (i.e. one for each month of the spawning season) that share a common covariance function (same $\kappa$ and $\tau$). This structure would highlight that the spawning areas are in different zones each month of the spawning season (Paradinas et al., 2015).

In the second and third cases:

$$u_{ij} = w_i + v_j$$

with $w_i$ a unique spatial realisation and $v_j$ being either a linear random effect (case 2) or a linear temporal trend effect (case 3) on the months. Case 2 would highlight that spawning areas are persistent during the months of the spawning season (Paradinas et al., 2015) and case 3, that they persist with an intensity trend over months of the spawning period (Paradinas et al., 2016).

Building from earlier model development, the inter-annual variability was added in our analysis as a linear random effect. First, as an independent variable:

$$u_{ijk} = w_i + v_j + x_k$$

with $w_i$ a unique spatial realisation, $v_j$ and $x_k$ two linear random effects, for the months and the years, respectively. This structure would highlight that spawning areas persist among months (like previous structure, case 1) but also among years during the spawning season.

Then, as a shared variable for the intra- and inter-annual variability with x levels (i.e. x spawning months × x years analysed):

$$u_{ijk} = w_i + v_{jk}$$

with $w_i$ a unique spatial realisation and $v_{jk}$ a linear random effect for the month $j$ of the year $k$. This structure would highlight a persistent pattern in seabass spawning areas distribution with small differences between month and years.

### 2.2.4 | Model evaluation

Models were calibrated using 75% of the dataset. INLA outputs propose the use of the Watanabe–Akaike information criterion (WAIC) to evaluate and compare the different combinations. This criterion computes the variance separately for each data point and averages after. It was preferred to the deviance information criterion (DIC), which only averages the variance over a point estimate. The prediction quality of the model was tested using cross-validation over the average logarithm of the conditional predictive ordinate (CPO; Geisser, 1993). The smaller the value of LCPO and WAIC, the better the compromise between fit, predictive quality and parsimony of the model. Hence, the best model was the one with the lowest LCPO and WAIC values. We also validated the best model on the remaining 25% of our dataset by mapping the predictions *vs*. the observations per month of the spawning season and per year. We finally used boxplots between observations and predictions to assess the ability of the model to predict values of 0 (absence) or 1 (presence).

### 2.2.5 | Model selection strategy

First, we selected the best spatio-temporal structure for each area. We then tested each covariate, together with the selected spatio-temporal structure, as a linear or non-linear (random walk 1 model) predictor, and chose the one that minimised our two criteria. For the covariates available at different depth levels in the water column (i.e.

**TABLE 1** Geometrical sets identified as hotspots of the CPUE spatial distribution for the English Channel for each month between 2008 and 2014

| | 2008 | 2009 | 2010 | 2011 | 2012 | 2013 | 2014 |
|---|---|---|---|---|---|---|---|
| January | $A_5^*$ | $A_5^*$ | $A_6^*$ | $A_5^*$ | $A_5^*$ | $A_6^*$ | $A_4$ |
| February | $A_5^*$ | $A_5^*$ | $A_5^*$ | $A_6^*$ | $A_5^*$ | $A_6^*$ | $A_2$ |
| March | $A_5^*$ | $A_5^*$ | $A_6^*$ | $A_5^*$ | $A_5^*$ | $A_6^*$ | $A_3$ |
| April | $A_5^*$ | $A_5^*$ | $A_5^*$ | $A_5^*$ | $A_5^*$ | $A_5^*$ | $A_5^*$ |
| May | $A_3$ | $A_3$ | $A_3$ | $A_3$ | $A_3$ | $A_5^*$ | $A_3$ |
| June | $A_3$ | $A_3$ | $A_3$ | $A_3$ | $A_3$ | $A_2$ | $A_2$ |
| July | $A_3$ | $A_3$ | $A_2$ | $A_3$ | $A_2$ | $A_2$ | $A_1$ |
| August | $A_2$ | $A_2$ | $A_2$ | $A_4$ | $A_2$ | $A_2$ | $A_2$ |
| September | $A_2$ | $A_2$ | $A_3$ | $A_2$ | $A_2$ | $A_2$ | $A_1$ |
| October | $A_3$ | $A_3$ | $A_2$ | $A_2$ | $A_2$ | $A_2$ | $A_2$ |
| November | $A_4$ | $A_4$ | $A_5^*$ | $A_4$ | $A_3$ | $A_5^*$ | $A_2$ |
| December | $A_6^*$ | $A_6^*$ | $A_5^*$ | $A_5^*$ | $A_5^*$ | $A_4$ | $A_2$ |

*Represent the two sets with the highest cut-off values.

temperature, salinity and current velocity), we selected the level with the lowest two criteria to be used in further combinations. If the covariate did not decrease the WAIC and/or average values of the LCPO compared to the spatio-temporal structure alone, it was not used further in the model construction. Finally, we tested all the combinations of the covariates selected. For each area, we selected the best model as the one representing the best compromise between low WAIC and LCPO values and containing solely relevant variables (i.e. variables whose 95% confidence interval (CI) does not cover 0).

## 3 | RESULTS

### 3.1 | Seabass spawning season

We applied the geostatistical methodology to each month in each of the two areas and for the whole study period. The results for each of the four criteria are summarised in Table S3 for the English Channel and Table S4 for the Bay of Biscay.

Tables 1 and 2 summarise the geometrical sets (i.e. from the set $A_1$ that corresponds to a cut-off of 0.5 kg.h$^{-1}$ of seabass/month/square to the set $A_{10}$ for a cut-off of 1000 kg.h$^{-1}$ of seabass/month/square) representative of the hotspots of the mean CPUE distribution for each month between 2008 and 2014, in the two areas.

The cut-off value defining the geometrical sets that correspond to hotspots of the CPUE spatial distribution varies depending on years, months and areas from 1 kg.h$^{-1}$ ($A_2$) to 50 kg.h$^{-1}$ ($A_6$) of seabass/month/square. As expected, hotspots corresponding to the highest cut-off values ($A_5$ and $A_6$) occurred mostly during winter (i.e. asterisks in Tables 1 and 2) and were assumed to characterise the spawning aggregations of seabass. Assuming that fishery data do indeed accurately capture the spawning aggregations within a year and that these cut-offs were selected correctly, our results indicate that the spawning season occurs between December and April in the English Channel and between January and March in the Bay of Biscay.

After considering the gonado-somatic index of European seabass in our two areas, we removed December data from our

**TABLE 2** Geometrical sets identified as hotspots of the CPUE spatial distribution for the Bay of Biscay for each month between 2008 and 2014

| | 2008 | 2009 | 2010 | 2011 | 2012 | 2013 | 2014 |
|---|---|---|---|---|---|---|---|
| January | $A_3$ | $A_5^*$ | $A_6^*$ | $A_6^*$ | $A_5^*$ | $A_5^*$ | $A_4$ |
| February | $A_5^*$ | $A_5^*$ | $A_5^*$ | $A_5^*$ | $A_5^*$ | $A_5^*$ | $A_5^*$ |
| March | $A_5^*$ | $A_5^*$ | $A_5^*$ | $A_5^*$ | $A_4$ | $A_4$ | $A_3$ |
| April | $A_3$ | $A_4$ | $A_4$ | $A_3$ | $A_3$ | $A_2$ | $A_3$ |
| May | $A_3$ | $A_3$ | $A_5^*$ | $A_4$ | $A_2$ | $A_3$ | $A_2$ |
| June | $A_3$ | $A_3$ | $A_4$ | $A_3$ | $A_2$ | $A_3$ | $A_2$ |
| July | $A_3$ | $A_3$ | $A_3$ | $A_2$ | $A_2$ | $A_3$ | $A_2$ |
| August | $A_3$ | $A_2$ | $A_3$ | $A_2$ | $A_2$ | $A_2$ | $A_2$ |
| September | $A_4$ | $A_2$ | $A_3$ | $A_3$ | $A_3$ | $A_3$ | $A_2$ |
| October | $A_3$ | $A_4$ | $A_3$ | $A_3$ | $A_5^*$ | $A_4$ | $A_4$ |
| November | $A_3$ | $A_3$ | $A_2$ | $A_5^*$ | $A_4$ | $A_3$ | $A_4$ |
| December | $A_5^*$ | $A_3$ | $A_3$ | $A_4$ | $A_5^*$ | $A_4$ | $A_4$ |

*Represent the two sets with the highest cut-off values.

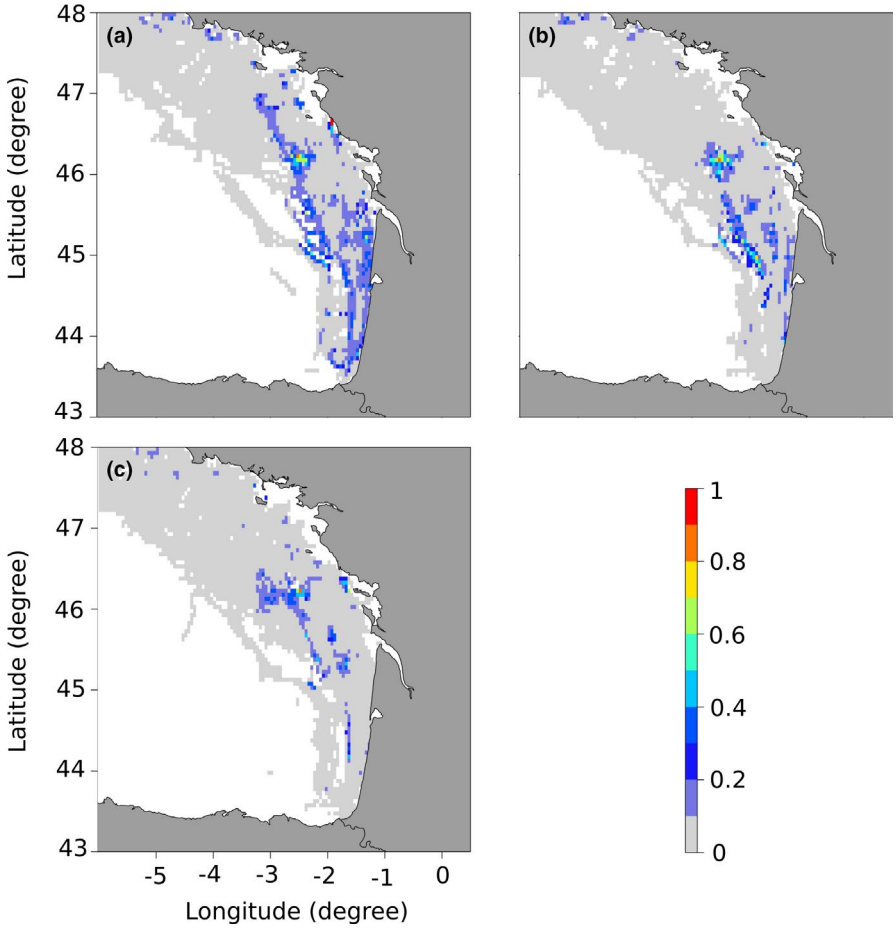


**FIGURE 3** Monthly average maps of seabass spawning areas, from the geostatistical analysis, in the Bay of Biscay during the period 2008–2013: (a) January, (b) February and (c) March. A probability of presence between 0 and 0.33 suggests that the area was rarely favourable every year. In contrast, a probability of presence between 0.66 and 1 indicates that the area was identified as a spawning area for several years. Values in between suggest that the area was occasionally favourable [Colour figure can be viewed at wileyonlinelibrary.com]

English Channel analysis, as we assumed that seabass would not be ready to spawn in this month. The seabass spawning season was then only slightly different between the two areas: from January to March in the Bay of Biscay and from January to April in the English Channel.

Besides, as the 2014 cut-off values were low compared to the other years (i.e. not surely highlighting spawning aggregations in winter), particularly in the English Channel, the next steps of our analyses only considered seabass' spawning areas identified over the period 2008–2013.

## 3.2 | Important spawning areas

Figures 3 and 4 represent average maps of hotspots during the spawning season.

In the Bay of Biscay (Figure 3), the Rochebonne Plateau (W 2°28, N 46°12) appeared as an essential spawning area during the entire spawning season (i.e. probability of presence as a spawning area between 0.5 and 0.8). Several occasional spawning areas also appeared along the continental shelf during the entire spawning season and particularly in February (i.e. probability between 0.2 and 0.4). Two additional occasional spots were found with lower probabilities (i.e. probability between 0.1 and 0.5): one in front of the Gironde Estuary (W 1°20, N 45°59) and another one west of Île de Ré (W 1°54, N° 46°21). Last, the Coast of the Landes (between N 44°60, N 43°50) appeared as an occasional spawning area at the beginning of the spawning season (i.e. probability between 0.1 and 0.5). The rest of the Bay of Biscay seems unfavourable for seabass reproduction, except in some specific areas in the west of Brittany (i.e. probability of presence as a spawning area between 0.1 and 0.3).

In the English Channel (Figure 4), the main spawning areas appeared more widespread. The North of the Cotentin peninsula (W 1°71, N 50°27) stood out as a stable spawning area throughout the spawning season (i.e. probability always above 0.6). One area in the south-west of Hampshire showed very high probability in March (probability >0.9, Figure 3). The Western English Channel appeared as a recurring spawning area, particularly in February (probability between 0.4 and 0.6). In contrast, the northeastern part of the English Channel showed more occasional and unfavourable areas for seabass reproduction.

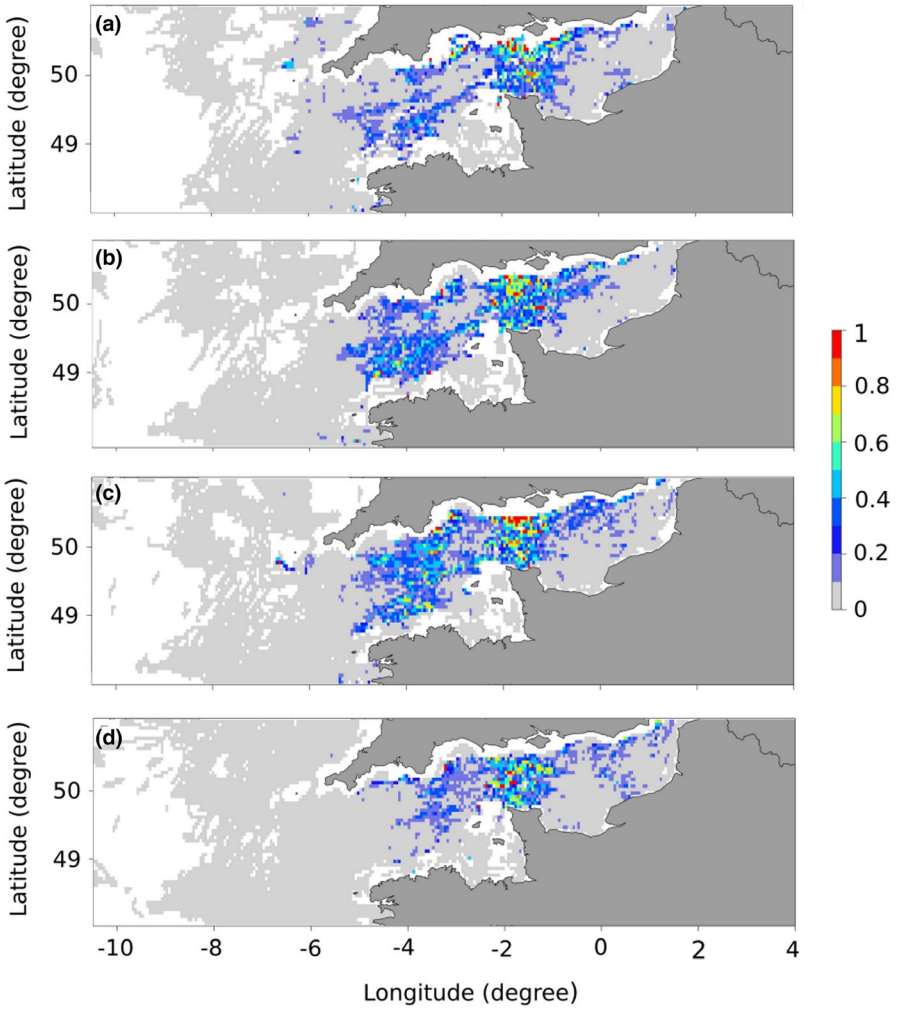


FIGURE 4 Monthly average maps of seabass spawning areas, from the geostatistical analysis, in the English Channel during the period 2008–2013: (a) January, (b) February, (c) March and (d) April. A probability of presence between 0 and 0.33 suggests that the area was rarely favourable every year. In contrast, a probability of presence between 0.66 and 1 indicates that the area was identified as a spawning area for several years. Values in between suggest that the area was occasionally favourable [Colour figure can be viewed at wileyonlinelibrary.com]

These figures show that the distribution of the spawning areas has shifted northward during the spawning season with (i) a decrease in their extent from January to March in the Bay of Biscay (see also Table 3) and (ii) a dome-shaped extent and a shift eastward between January and April in the English Channel (with a peak in February and March; Table 4).

We observed significant annual variability in the extent of the spawning areas in the Bay of Biscay with a trend towards smaller spawning areas in the latest years (Table 3). A similar pattern was observed for the English Channel (Table 4), with large annual variability and a trend towards smaller spawning areas over the series, at the exception of January and March 2011 and February and March 2012.

### 3.3 | Environmental drivers explaining the distribution of the spawning areas

The results of the five spatio-temporal structures are presented in Table 5. The best structure corresponds to a persistent spatial distribution with random intensity changing over months and years together (case 5) in the Bay of Biscay and the English Channel.

| | 2008 | 2009 | 2010 | 2011 | 2012 | 2013 | Mean | SD |
|---|---|---|---|---|---|---|---|---|
| January | 10,248 | 7779 | 926 | 1173 | 2963 | 2160 | 4208 | 3872 |
| February | 5031 | 2438 | 2068 | 1728 | 1481 | 1605 | 2392 | 1339 |
| March | 3611 | 926 | 802 | 1389 | 1450 | 1697 | 1646 | 1020 |

TABLE 3 The extent of the spawning areas ($km^2$) for each month of the spawning season in the Bay of Biscay as deduced from the number of squares of three nautical miles highlighted as a spawning area

**TABLE 4** The extent of the spawning areas ($km^2$) for each month of the spawning season in the English Channel–Celtic Sea as deduced from the number of squares of three nautical miles highlighted as a spawning area

| | 2008 | 2009 | 2010 | 2011 | 2012 | 2013 | Mean | SD |
|---|---|---|---|---|---|---|---|---|
| January | 12,100 | 7130 | 7748 | 13,829 | 8828 | 5463 | 9183 | 3173 |
| February | 15,619 | 18,428 | 13,613 | 6050 | 15,125 | 5463 | 12,383 | 5367 |
| March | 13,952 | 19,262 | 8519 | 14,909 | 16,360 | 10,094 | 13,849 | 3981 |
| April | 8519 | 10,649 | 6575 | 5402 | 4043 | 11,915 | 7851 | 3063 |

**TABLE 5** WAIC and mean LCPO values for the five tested spatio-temporal structures

| | | English Channel | | Bay of Biscay | |
|---|---|---|---|---|---|
| Spatio-temporal structure | Process | WAIC | LCPO | WAIC | LCPO |
| $u_{ij} = w_{ij}$ | Opportunistic monthly spatial distribution during the spawning season | 78,589 | 0.2970 | 12432 | 0.1048 |
| $u_{ij} = w_i + v_j\,(1)$ | Persistent spatial distribution with random intensity changes over the months of the spawning season | 32,178 | 0.1216 | 8215 | 0.068 |
| $u_{ij} = w_i + v_j\,(2)$ | Persistent spatial distribution with temporal intensity trend over the months of the spawning season | 77,614 | 0.2934 | 11862 | 0.096 |
| $u_{ijk} = w_i + v_j + x_k$ | Persistent spatial distribution with random intensity changes over months and years separately | 31,995 | 0.1209 | 7648 | 0.0642 |
| $u_{ijk} = w_i + v_{jk}$ | Persistent spatial distribution with random intensity changes over months and years together | 31,344 | 0.1185 | 7526 | 0.0636 |

The results of all linear combinations are presented in Table S5 (English Channel) and S6 (Bay of Biscay). We removed from the final model covariates whose 95% CI included zero (i.e. the intercept and the chlorophyll-*a* in the English Channel and the intercept and the bottom grain size in the Bay of Biscay). Thus, the best models were:

$$g^{-1}\left(\pi_{ijk}\right) = \beta_1 \mathrm{Mld} + \beta_2 \mathrm{UoVo}\, S + f(\mathrm{mean}S) + f(\mathrm{mean}T) + w_i + v_{jk}$$

in the English Channel and:

$$g^{-1}\left(\pi_{ijk}\right) = \beta_1 \mathrm{Bathy} + \beta_2 \mathrm{Mld} + f(\mathrm{mean}T) + w_i + v_{jk}$$

in the Bay of Biscay.

Figure 5 shows an example of the validation using the remaining 25% of our dataset, in each area (for January 2008). All predictions over the time series are provided in supplementary materials (Figures S4 and S5).

The models were efficient in predicting the general pattern of presence of the spawning areas but did not accurately predict their precise location (see low probabilities in Figure 5). This is confirmed in Figure 6, which shows that the models can detect unfavourable and favourable areas. Yet, for the later, the probabilities remain lower than expected, and we would have expected, a better ability to discriminate favourable areas (i.e. probability closer to 1).

Table 6 shows that both covariates (current velocity and mixed layer depth) have a positive effect on the distribution of the spawning areas in the English Channel. In the Bay of Biscay, bathymetry also has a positive effect, while mixed layer depth has a negative effect.

Figure 7 illustrates the non-linear effect of each environmental covariate on the probability of the presence of seabass spawning areas as predicted by the best model in the English Channel. According to these results, seabass prefer locations with a mixed layer depth between 50 and 90 m, with moderate currents (mostly between 0.15 and 0.17 $m.s^{-1}$), and temperature around 10°C and avoid temperatures around 7°C, they also avoid salinity around 34.

Figure 8 shows the effect of the covariates in the Bay of Biscay. Seabass target areas between 30 and 90 m deep, a mixed layer depth of 100 m and shallower, and temperatures around 9–10°C and avoid temperatures around 13°C.

The spatial effect nominal range, the variances of the spatio-temporal effect and the temporal structure are illustrated in Figures S6 (English Channel) and Figures S7 (Bay of Biscay). The mean posterior value of the spatial effect nominal range (i.e. the mean diameter of the spawning areas) is around 170 km in the English Channel and 120 km in the Bay of Biscay. The scale of the variances for the spatial and temporal structures is similar from an area to another, with the spatial variances being smaller than the temporal variances. The Gaussian field with Matérn correlation, named the spatial field, is

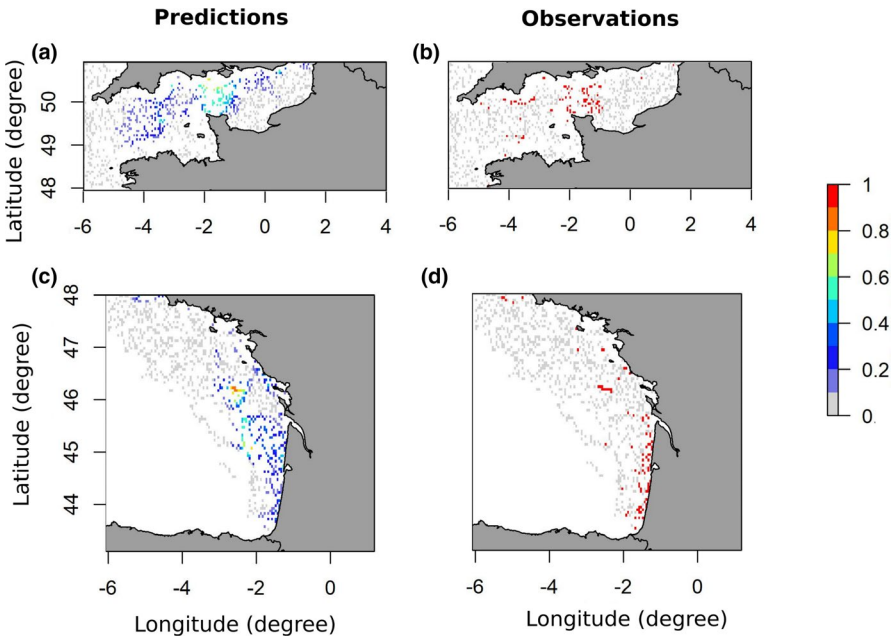


FIGURE 5 Predicted maps of probabilities for the presence of seabass spawning areas in January 2008 for the English Channel (a & b) and the Bay of Biscay (c & d) with the best spatio-temporal model compared to the maps of observed seabass spawning areas [Colour figure can be viewed at wileyonlinelibrary.com]

rather smooth, while most of the variability is temporal (intra- and inter-annual).

In the English Channel, the random intensity changes (Figure S6, C) remain very variable across years. In average, random intensity is high for February and March and low for January and April. In the Bay of Biscay (Figure S7, C), the variability of the spatial field during the spawning season moves from high in January to low in March except for years 2010 and 2011 showing higher values in February than in January.

The mean and standard deviation of the persistent spatial field are shown in Figures S8 (English Channel) and Figures S9 (Bay of Biscay). From the values of the posterior mean of the spatial effect, the spatial field itself can locate most of the areas favourable for reproduction. The contribution of each covariate to the prediction ability of the model (Tables 7 and 8) also confirms the importance of the spatial field. In both areas, removing the spatio-temporal structure leads to a model with weak prediction skills (i.e. less than 1% combined). In the English Channel, the spatial structure seems to explain more than the temporal structure, whereas this is the opposite in the Bay of Biscay. In both cases, the environmental covariates do not explain much of the seabass spawning distribution.

## 4 | DISCUSSION

The ecology of the wild seabass reproduction is an important research focus for fishery scientists. Reproduction is a critical phase of fish life cycles for population renewal. It is also a phase when a species is most vulnerable to overexploitation as fish aggregate in

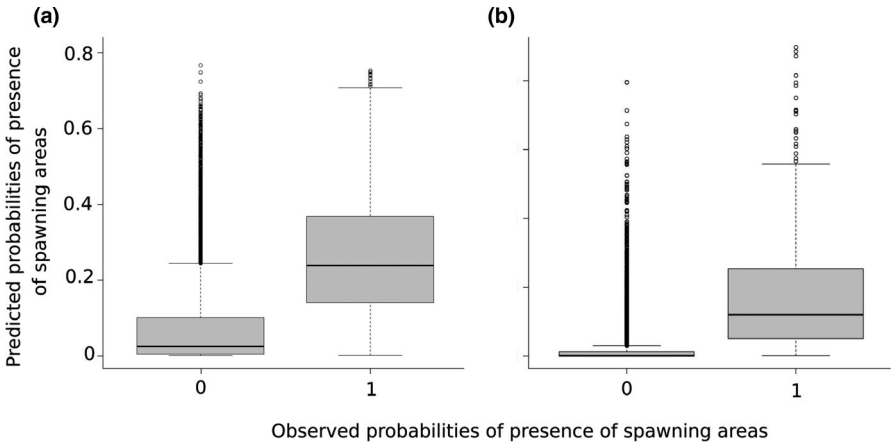


FIGURE 6 Predicted probabilities of presence of seabass spawning areas vs observed seabass spawning areas with the best spatio-temporal model for (a) the English Channel and (b) the Bay of Biscay

**TABLE 6** Summary of the fixed effects of the best model for the English Channel (two first lines) and the Bay of Biscay (two last lines)

| Fixed effect | Mean | SD | 25% Q | 97.5% Q |
|---|---|---|---|---|
| Mld | 0.006 | 0.002 | 0.002 | 0.009 |
| UoVoS | 3.931 | 0.894 | 2.170 | 5.681 |
| Bathy | 0.003 | 0.001 | 0.0009 | 0.006 |
| Mld | −0.005 | 0.002 | −0.009 | −0.0008 |

restricted areas. By sampling eggs and larvae in the English Channel, several studies revealed that seabass reproduce mainly offshore (e.g. Thompson & Harrop, 1987) but that coastal spawning areas also exist (e.g. Kennedy & Fitzmaurice, 1972). Tagging surveys have also confirmed the migration of seabass to offshore spawning areas (Pawson et al., 2007) and highlighted their fidelity to these areas (de Pontual et al., 2019). Managing these areas is therefore critical for the sustainability of seabass populations.

Unlike for many other species such as cod (Andrews et al., 2006) or hake (Woillez et al., 2007), no quantitative spatial observation independent from fishery data (i.e. scientific survey) occurred in winter to characterise European seabass spawning distribution in the North Atlantic. Only fishermen's knowledge can locate them qualitatively, and fishery data were the only data available for our study. Therefore, we made the hypothesis that these data would be suitable to capture seabass spawning areas as well as the timing of spawning.

However, CPUE data are known to be non-proportional to fish abundance. The two main types of non-proportionality have been reviewed by Harley et al. (2001): (i) hyperstability, which is the most common (i.e. CPUE declines slower than abundance, as observed when fishing effort is concentrated on large fish aggregations), and (ii) hyperdepletion (i.e. CPUE declines faster than abundance, due to different fish behaviour in response to fishing gear). In our study, ignoring CPUE hyperstability in seabass spawning areas could lead to erroneous conclusions about the abundance of the species. We acknowledged the possible biases in our results due to catchability and efficiency differences and changes over time for this multi-gear fishery. However, our objective was to study seabass aggregation behaviour rather than modelling and mapping their abundance. The spatial structure of the tail of the CPUE distribution (i.e. that of a cut-off at high CPUE values) was thus still very informative to indicate spawning aggregations. Besides, fishermen prospecting only known fishing areas have access to limited fish quantities, and some secondary spawning areas may be unnoticed (e.g. in the coastal zone, where VMS based fishing distribution is lower, see Figure 1). There are also differences in fishing efficiency between gears or catchability

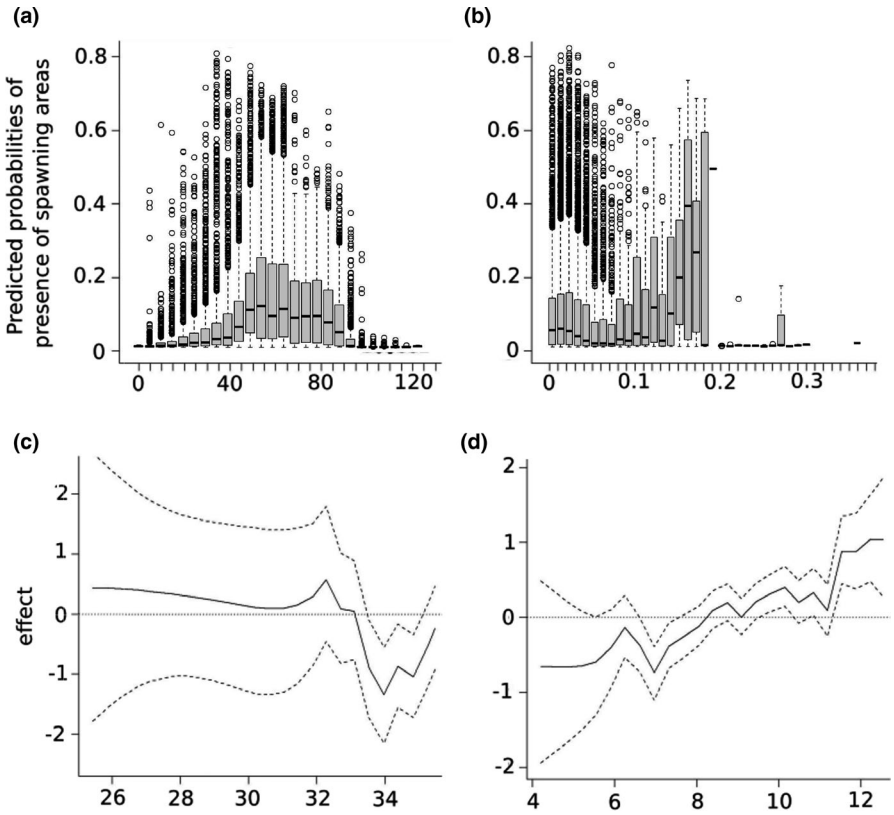


**FIGURE 7** Predicted probabilities of presence with the best model in the English Channel under (a) mixed layer depth, (b) surface current velocities, (c) mean salinity of the water column and (d) mean temperature of the water column. For (a) and (b), each boxplot corresponds to an interval of 5 m for the mixed layer depth and 0.01 $m.s^{-1}$ for current velocities. The rectangles go from the first to the third quartiles and are cut by a horizontal line, which represents the median. The whiskers lead to the outliers, which are represented by dots. For (c) and (d), dotted lines represent the 25% and 95% quantiles

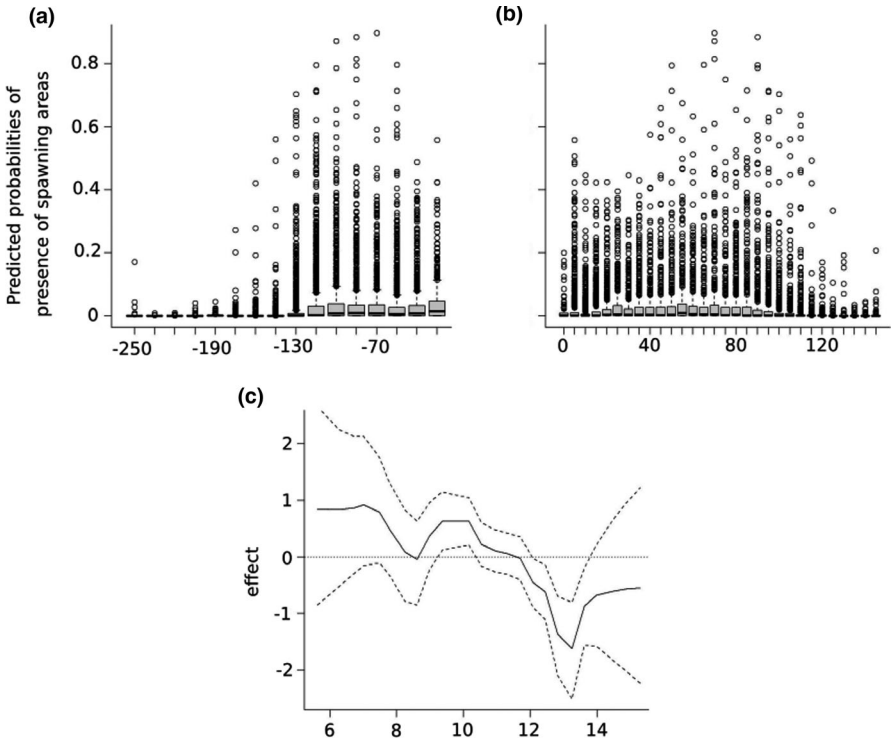


**FIGURE 8** Predicted probabilities of presence with the best model in the Bay of Biscay under (a) bathymetry, (b) mixed layer depth and (c) mean temperature of the water column. For (a) and (b), each boxplot corresponds to an interval of 15 m for the bathymetry and 5 m for the mixed layer depth. The rectangles go from the first to the third quartiles and are cut by a horizontal line, which represents the median. The whiskers lead to the outliers, which are represented by dots. For (c), dotted lines represent the 25% and 95% quantiles

between fishermen. The detection of core spawning areas may be compromised by fishermen who overestimate the importance of secondary spawning aggregations. However, as pelagic trawlers are the main fleet targeting seabass aggregations in winter, and also the most efficient fleet to catch spawning seabass (see Figures S2 and S3), we believe core spawning areas are correctly detected, while secondary spawning areas may be underestimated or missed (e.g. exploited by a less efficient gear, e.g. gillnets). Then, as the gear composition over space did not change substantially over the period, we considered that our analysis was weakly impacted by the changes in fishing efficiency over time. Our two stage analysis does not account for the differences in fishing effort, and fishermen may conduct more fishing operations in areas with high fish abundance. By aggregating CPUE data over squares and months, preferential sampling should result in higher average CPUE in areas with high fish abundance. As the full range of CPUE values is used to predict the spatial distribution of abundance or biomass, our non-linear geostatistics approach allows us to focus on the most productive areas without trying to correct for biases or errors due to differences in catchability.

With this approach, we have identified the recurring spawning areas of the European seabass along the French Atlantic coast. Our average maps of the presence of spawning areas are in line with fishermen's empirical knowledge of seabass spawning areas (Drogou, pers. comm.). We also confirmed the persistence of their distribution across months and years using a Bayesian spatio-temporal analysis. We identified three key spawning areas throughout the reproductive season: the Rochebonne Plateau in the Bay of Biscay, the Western English Channel and the North of the Cotentin Peninsula in the eastern English Channel. These results are congruent with the work of Masski (1998), who highlighted significant seabass abundance in the Western English Channel from January to April. Our study is also in agreement with Fritsch (2005), who pointed out to two recurring areas in the Bay of Biscay: the Rochebonne Plateau and the south of the Gironde Estuary. However, the author pointed out the significant variations in seabass aggregations across years in this area. Our study provides critical information for seabass fishery management in the North Atlantic. However, a dedicated scientific survey during the spawning season could improve knowledge on seabass reproduction and provide more information on the spatial distribution and maturity of adults, as well as on the number and stages of eggs.

We also identified a northeast gradient in the occurrence of spawning areas, which changes over time: spawning areas progress northward from the southern section of the Bay of Biscay to the middle of the English Channel during the spawning season. This result is consistent with the work of Thompson and Harrop (1987), who described an eastward gradient of occurrence in the spawning areas of the English Channel from February to the end of June. Our Bayesian spatio-temporal analysis confirmed this result by showing: (i) a seasonal trend with a decrease in the number of spawning areas throughout the spawning season particularly in the Bay of Biscay;

**TABLE 7** Contribution of each covariate to the model predictive skills in the English Channel

| Model | LCPO | Relative variation (%) |
|---|---|---|
| Entire model | 0.1175629 | 0 |
| Model without temporal structure | 0.1238289 | 5.33 |
| Model without spatial structure | 0.1771387 | 50.68 |
| Model without spatio-temporal structure | 0.2155217 | 83.32 |
| Model without mean S | 0.1178772 | 0.27 |
| Model without mean T | 0.117961 | 0.34 |
| Model without Mld | 0.1176035 | 0.03 |
| Model without UoVoS | 0.1176306 | 0.06 |

**TABLE 8** Contribution of each covariate to the model predictive skills in the Bay of Biscay

| Model | LCPO | Relative variation (%) |
|---|---|---|
| Entire model | 0.0582153 | 0 |
| Model without temporal structure | 0.08210038 | 41.03 |
| Model without spatial structure | 0.07460561 | 28.15 |
| Model without spatio-temporal structure | 0.09887661 | 69.85 |
| Model without Bathy | 0.05837433 | 0.27 |
| Model without mean T | 0.05854458 | 0.57 |
| Model without Mld | 0.0584373 | 0.38 |

and (ii) a non-significant inter-annual variability in the importance of the spatial field for each month of the spawning season.

Unfortunately, the geostatistical method, even if it presents higher cut-offs in winter, does not allow characterising precisely the seabass' spawning season. Indeed, a latitudinal gradient in the beginning of the spawning season is known (e.g. Vinagre et al., 2009), which does not appear in our analysis. Based on only one available study that was conducted almost two decades ago (Pawson & Pickett, 1996), we removed December from our analysis in the English Channel as it could rather represent pre-spawning aggregations (Vázquez and Muñoz-Cueto, 2014) or a shift in the spawning period due to climate change compared to the study. Moreover, we had to remove the year 2014 from our analysis. The low cut-off value observed could be linked to particularly bad weather conditions that impaired French pair trawlers to fish this year (ICES, 2015). However, it could also be linked to changes in the abundance of the species. Indeed, as explained by Petitgas (1998), the level of fish aggregation can be associated with seabass biomass and the lower cut-off value could reflect lower biomass in 2014. This is in agreement with the 2015 ICES report, which highlights a decrease in the northern seabass spawning stock biomass (SSB) since 2013.

Combining our hotspot detection results and those of the gonado-somatic index, we showed that the seabass spawning season ends earlier in the Bay of Biscay than in the English Channel. This result is congruent with the work of Vinagre et al. (2009) showing a latitudinal gradient in the seabass spawning season. However, using our methodology, it was difficult to characterise the exact timing of the spawning season, even if cut-offs appeared lower in spring and summer than in winter and autumn. One way to improve the hotspot methodology for characterising the timing of the seabass spawning season using VMS data only could be the implementation of monthly cross-variograms and the study of the correlation between geometrical sets at different spatial scales. This method could help to highlight how seabass aggregations form, persist and disappear throughout the spawning season. Moreover, we decomposed our analysis in two parts but according to Opitz et al. (2018), threshold overrun and environmental predictors could be combined in one modelling approach within INLA.

Our Bayesian spatio-temporal models suggest that the spatio-temporal effect explains most of the distribution of seabass spawning areas. Using a correlative approach, we found that it was difficult to predict seabass spawning areas using the selected environmental variables as they did not explained much of the presence/absence of seabass' spawning areas. The underlying ecological process driving the geographical distribution of seabass spawning areas is not elucidated by available environmental covariates. According to de Pontual et al. (2019), we can expect that seabass return to the same spawning areas. Two non-exclusive processes can explain this fidelity behaviour. One is the possibility of a stock memory to ensure good population renewal, referred to as the 'Entrainment hypothesis' (Petitgas et al., 2006). In the 'Entrainment hypothesis', first-time spawners learn the migration routes from old adults to ensure the spatial persistence and the closure of their life cycle. The second is the homing process (Griffin, 1953) in which fish have the innate ability to go and reproduce where they were born. This process could explain the persistence of seabass spawning areas. The question of natal homing could be addressed using near-core otolith microchemistry analysis, as done for several other species (e.g. Artetxe-Arrate et al., 2019). Testing these hypotheses using a mechanistic approach could help identify the environmental forcing characterising the distribution pattern of seabass spawning areas.

For the covariates, our models showed that environmental drivers poorly explained seabass distribution. In both areas, temperature over the water column and mixed layer depth have been selected. In addition, mean salinity of the water column and currents of the surface have been selected in the English Channel, while bathymetry has been selected in the Bay of Biscay. It is difficult to discuss seabass preferences, as covariates do not explain more than 1% of the spawning areas distribution. We thus averaged the value of the covariates selected in each areas during the spawning season for spawning and feeding (i.e. areas at less than 5 km from the coast; e.g. Pawson et al., 2007) areas to gain some knowledge on the species ecology. It indicates that, in the English

Channel, seabass tend to prefer for reproduction waters with salinity around 35.4 (vs 34.3 for feeding), temperature around 9.4°C (vs 8.8°C), currents around 0.03 $m.s^{-1}$ (vs 0.04 $m.s^{-1}$) and a mixed layer depth around 59 m (vs 18 m). In the Bay of Biscay, seabass tend to prefer for reproduction temperature around 11.3°C (vs 10.1°C for feeding), mixed layer depth around 57 m (vs 16 m) and bathymetry around 82 m (vs 23 m). Higher salinity, bathymetry and mixed layer depth in spawning areas agree with the offshore winter migrations observed by Pawson et al. (2007) and de Pontual et al. (2019). Adult seabass target coastal areas to feed, because they are rich in food. However, environment in those areas is highly variable (e.g. salinity and temperature) resulting in a high energy cost for the species. In winter, when temperatures near the coast drop, it is likely that they move from these areas to the open sea and invest all their stored energy in reproduction. Indeed, Pickett and Pawson (1994) identified temperature as the main factor leading to the migration of seabass. Our results tend to confirm this assumption, with seabass targeting areas around 11°C in the Bay of Biscay and areas slightly colder (around 9°C) in the English Channel. These results are in agreement with Pawson et al. (2007) who showed that adult seabass might be migrating to seek warmer water (>9°C) in the English Channel, and de Pontual et al. (2019) who found that seabass rarely spent time below 9°C.

Some other limits are worth to notice. The assumptions of the SACROIS flow on the quantity of the species per square are debatable. Indeed, the flow recalculates the position of the fishing events from the VMS data (NB: a vessel is considered to be fishing below 5 knots) to reallocate the fish quantity during the days at sea. The quantity sold at the end of a fishing trip is reallocated homogenously and proportionally to the fishing duration, as averaged across all fishing events, thus smoothing the data. The values of the two gonado-somatic index used to check the timing of the seabass spawning season are also debatable. Indeed, their value came from studies conducted over one year, while Fritsch (2005) shows that fish maturity depends on environmental conditions and individual morphology, which can vary from year to year. This author also showed that the seabass spawning period as identified using the gonado-somatic index is relatively stable across years in the English Channel. We assumed that the situation was similar in the Bay of Biscay, but further studies are needed to confirm this hypothesis.

Finally, Harden Jones (1968) suggested that returning to the same spawning areas to ensure successful egg and larval drift could be a selective advantage. It is therefore essential to assess if fish consistently spawn in the same areas over time to maximise spawning efficiency and recruitment. If recruitment is a dominant factor in seabass population's dynamics, it would help to manage the fished populations. Due to the high inter-annual variability, it would also be relevant to study which areas contribute most to population renewal. Understanding the relationship between the adult stock and recruits is very challenging in fishery science because of high inter-annual variability due to many poorly understood factors (Houde, 2008). A popular tool to study the pelagic larval phase of fish is a spatially explicit individual-based model (IBM). Beraud et al. (2018) developed this approach to study the settlement success of European seabass larvae under different hydrological conditions in the English Channel. Combining it to bioenergetics (e.g. Dambrine et al., 2020) would make it possible to take into account the different growth patterns under various environmental conditions. Doing this could help to understand the connectivity between offshore spawning areas and coastal nurseries and provide valuable knowledge for better assessing stock–recruitment relationship and improve fishery management. Characterising and understanding the connectivity between spawning areas and nurseries could help developing better management practices (e.g. areas with monthly fishing ban) and design relevant protected areas.

## ACKNOWLEDGEMENTS

This study was part of the Barfray project funded by the European Maritime and Fisheries Fund (EMFF-OSIRIS N°: PFEA 400017DM0720006), France Filière Pêche (FFP), the French Ministry of Agriculture and Food (MAF) and Ifremer. The authors are grateful to the Direction des pêches maritimes et de l'aquaculture (DPMA) and Ifremer (Système d'Informations Halieutiques) who provided the aggregated VMS data. The findings and conclusions of the present paper are those of the authors. This study was conducted using E.U. Copernicus Marine Service Information to collect covariate data. The authors finally thank two anonymous reviewers for their constructive comments that helped to improve the manuscript significantly.

## CONFLICT OF INTEREST

The authors have no conflict of interest to declare.

## AUTHOR CONTRIBUTIONS

CD, MW, MH and HdP conceived the research idea; CD ran data analyses and wrote the manuscript; and MW, MH and HdP participated in discussions of the results and critically reviewed the manuscript.

## DATA AVAILABILITY STATEMENT

Research data are not shared.

## ORCID

*Chloé Dambrine* https://orcid.org/0000-0002-2386-3808

## REFERENCES

Andrews, J. M., Gurney, W. S., Heath, M. R., Gallego, A., O'Brien, C. M., Darby, C., & Tyldesley, G. (2006). Modelling the spatial demography of Atlantic cod (*Gadus morhua*) on the European continental shelf. *Canadian Journal of Fisheries and Aquatic Sciences*, *63*(5), 1027–1048. https://doi.org/10.1139/f06-006

Artetxe-Arrate, I., Fraile, I., Crook, D. A., Zudaire, I., Arrizabalaga, H., Greig, A., & Murua, H. (2019). Otolith microchemistry: a useful tool for investigating stock structure of yellowfin tuna (*Thunnus albacares*) in the Indian Ocean. *Marine and Freshwater Research*, *70*(12), 1708–1721. https://doi.org/10.1071/MF19067

Bakka, H., Rue, H., Fuglstad, G.-A., Riebler, A., Bolin, D., Illian, J., Krainski, E., Simpson, D., & Lindgren, F. (2018). Spatial modeling with R-INLA:

A review. *Wiley Interdisciplinary Reviews: Computational Statistics*, *10*(6), e1443. https://doi.org/10.1002/wics.1443

Bartolino, V., Maiorano, L., & Colloca, F. (2011). A frequency distribution approach to hotspot identification. *Population Ecology*, *53*(2), 351–359. https://doi.org/10.1007/s10144-010-0229-2

Bellido, J. M., Brown, A. M., Valavanis, V. D., Giráldez, A., Pierce, G. J., Iglesias, M., & Palialexis, A. (2008). Identifying essential fish habitat for small pelagic species in Spanish Mediterranean waters. *Essential Fish Habitat Mapping in the Mediterranean* (pp. 171–184). Dordrecht, The Netherlands: Springer.

Beraud, C., van der Molen, J., Armstrong, M., Hunter, E., Fonseca, L., & Hyder, K. (2018). The influence of oceanographic conditions and larval behaviour on settlement success—the European sea bass Dicentrarchus labrax (L.). *ICES Journal of Marine Science*, *75*(2), 455–470. https://doi.org/10.1093/icesjms/fsx195

Brodie, S., Hobday, A. J., Smith, J. A., Everett, J. D., Taylor, M. D., Gray, C. A., & Suthers, I. M. (2015). Modelling the oceanic habitats of two pelagic species using recreational fisheries data. *Fisheries Oceanography*, *24*(5), 463–477. https://doi.org/10.1111/fog.12122

Colloca, F., Bartolino, V., Lasinio, G. J., Maiorano, L., Sartor, P., & Ardizzone, G. (2009). Identifying fish nurseries using density and persistence measures. *Marine Ecology Progress Series*, *381*, 287–296. https://doi.org/10.3354/meps07942

Dahlgren, C. P., Kellison, G. T., Adams, A. J., Gillanders, B. M., Kendall, M. S., Layman, C. A., Ley, J. A., Nagelkerken, I., & Serafy, J. E. (2006). Marine nurseries and effective juvenile habitats: concepts and applications. *Marine Ecology Progress Series*, *312*, 291–295. https://doi.org/10.3354/meps312291

Dambrine, C., Huret, M., Woillez, M., Pecquerie, L., Allal, F., Servili, A., & De Pontual, H. (2020). Contribution of a bioenergetics model to investigate the growth and survival of European seabass in the Bay of Biscay-English Channel area. *Ecological Modelling*, *423*, 109007. https://doi.org/10.1016/j.ecolmodel.2020.109007

de Pontual, H., Lalire, M., Fablet, R., Laspougeas, C., Garren, F., Martin, S., Drogou, M., & Woillez, M. (2019). New insights into behavioural ecology of European seabass off the West Coast of France: implications at local and population scales. *ICES Journal of Marine Science*, *76*(2), 501–515. https://doi.org/10.1093/icesjms/fsy086

Demanèche, S., Bégot, E., Gouello, A., Habasque, J., Merrien, C., Leblond, E., Berthou, P., Harscoat, V., Fritsch, M., Leneveu, C., & Laurans, M. (2010). *Projet SACROIS "IFREMER/DPMA" - Rapport final. Convention SACROIS, 2008–2010*.

Domeier, M. L. (2012). Revisiting spawning aggregations: definitions and challenges. In: Y. Sadovy de Mitcheson, & P. Colin (Eds), *Reef fish spawning aggregations: biology, research and management*. Fish & Fisheries Series, vol *35*. Springer, Dordrecht.

Fritsch, M. (2005). *Traits biologiques et exploitation du bar commun Dicentrarchus labrax (L.). dans les pêcheries françaises de la Manche et du golfe de Gascogne* (Doctoral dissertation. Université de Bretagne Occidentale).

Geisser, S. (1993). *Predictive inference: An introduction*. London: Chapman and Hall.

Griffin, D. R. (1953). Sensory physiology and the orientation of animals. *American Scientist*, *41*(2), 208–281.

Hamdi, A., Vasquez, M., & Populus, J. (2010). *Cartographie des habitats physiques EUNIS - Côtes de France*. Convention Ifremer/AAMP, n° 09/12177764/FY.

Harden Jones, F. R. (1968). *Fish migration* (p. 325). London: Edward Arnold Ltd.

Harley, S. J., Myers, R. A., & Dunn, A. (2001). Is catch-per-unit-effort proportional to abundance? *Canadian Journal of Fisheries and Aquatic Sciences*, *58*(9), 1760–1772. https://doi.org/10.1139/f01-112

Heerah, K., Woillez, M., Fablet, R., Garren, F., Martin, S., & De Pontual, H. (2017). Coupling spectral analysis and hidden Markov models for the segmentation of behavioural patterns. *Movement Ecology*, *5*(1), 1–15. https://doi.org/10.1186/s40462-017-0111-3

Hintzen, N. T., Bastardie, F., Beare, D., Piet, G. J., Ulrich, C., Deporte, N., Egekvist, J., & Degel, H. (2012). VMStools: Open-source software for the processing, analysis and visualisation of fisheries logbook and VMS data. *Fisheries Research*, *115*, 31–43. https://doi.org/10.1016/j.fishres.2011.11.007

Houde, E. D. (2008). Emerging from Hjort's shadow. *Journal of Northwest Atlantic Fishery Science*, *41*, 53–70.

ICES. (2012). *Report of the Working Group for the Celtic Seas Ecoregion (WGCSE)*, 9–18 May 2012, Copenhagen, Denmark. ICES CM 2012/ACOM:12. 1715 pp.

ICES. (2015). *Report of the Working Group for the Celtic Seas Ecoregion (WGCSE)*, 12–21 May 2015, Copenhagen, Denmark. ICES CM 2015/ACOM:12. 1432 pp.

ICES. (2018). *Report of the Working Group on Celtic Seas Ecoregion (WGCSE)*, 9–18 May 2018, Copenhagen, Denmark. ICES CM 2018/ACOM:13. 1887 pp.

Kennedy, M., & Fitzmaurice, P. (1972). The biology of the bass, Dicentrarchus labrax, in Irish waters. *Journal of the Marine Biological Association of the United Kingdom*, *52*(3), 557–597. https://doi.org/10.1017/S0025315400021597

Kneib, T., Müller, J., & Hothorn, T. (2008). Spatial smoothing techniques for the assessment of habitat suitability. *Environmental and Ecological Statistics*, *15*(3), 343–364. https://doi.org/10.1007/s10651-008-0092-x

Large, P. A., Diez, G., Drewery, J., Laurans, M., Pilling, G. M., Reid, D. G., Reinert, J., South, A. B., & Vinnichenko, V. I. (2009). Spatial and temporal distribution of spawning aggregations of blue ling (*Molva dypterygia*) west and northwest of the British Isles. *ICES Journal of Marine Science*, *67*(3), 494–501. https://doi.org/10.1093/icesjms/fsp264

Lindgren, F., Rue, H., & Lindström, J. (2011). An explicit link between Gaussian fields and Gaussian Markov random fields: the stochastic partial differential equation approach. *Journal of the Royal Statistical Society: Series B (Statistical Methodology)*, *73*(4), 423–498. https://doi.org/10.1111/j.1467-9868.2011.00777.x

Magnuson-Stevens Fishery Act (2007). *Management Reauthorization Act of 2006*. Public Law. 479.

Martínez-Minaya, J., Cameletti, M., Conesa, D., & Pennino, M. G. (2018). Species distribution modeling: a statistical review with focus in spatio-temporal issues. *Stochastic Environmental Research and Risk Assessment*, *32*(11), 3227–3244. https://doi.org/10.1007/s00477-018-1548-7

Masski, H. (1998). *Identification des frayères et étude des structures de population du turbot Psetta maxima L. Et du bar Dicentrachus labrax L*. En Manche ouest et dans les zones avoisinantes (Doctoral dissertation. Brest).

Maunder, M. N., Sibert, J. R., Fonteneau, A., Hampton, J., Kleiber, P., & Harley, S. J. (2006). Interpreting catch per unit effort data to assess the status of individual stocks and communities. *Ices Journal of Marine Science*, *63*(8), 1373–1385. https://doi.org/10.1016/j.icesjms.2006.05.008

Munoz, F., Pennino, M. G., Conesa, D., López-Quílez, A., & Bellido, J. M. (2013). Estimation and prediction of the spatial occurrence of fish species using Bayesian latent Gaussian models. *Stochastic Environmental Research and Risk Assessment*, *27*(5), 1171–1180. https://doi.org/10.1007/s00477-012-0652-3

Nelson, T. A., & Boots, B. (2008). Detecting spatial hot spots in landscape ecology. *Ecography*, *31*(5), 556–566. https://doi.org/10.1111/j.0906-7590.2008.05548.x

Opitz, T., Huser, R., Bakka, H., & Rue, H. (2018). INLA goes extreme: Bayesian tail regression for the estimation of high spatio-temporal quantiles. *Extremes*, *21*(3), 441–462.

Paradinas, I., Conesa, D., Pennino, M. G., Muñoz, F., Fernández, A. M., López-Quílez, A., & Bellido, J. M. (2015). Bayesian spatio-temporal

approach to identifying fish nurseries by validating persistence areas. *Marine Ecology Progress Series*, *528*, 245–255. https://doi.org/10.3354/meps11281

Paradinas, I., Marín, M., Grazia Pennino, M., López-Quílez, A., Conesa, D., Gonzalez, M., & María Bellido, J. Handling editor: Ernesto Jardim. (2016). Identifying the best fishing-suitable areas under the new European discard ban. *ICES Journal of Marine Science*, *73*(10), 2479–2487. https://doi.org/10.1093/icesjms/fsw114

Pawson, M. G., & Pickett, G. D. (1996). The annual pattern of condition and maturity in bass, *Dicentrarchus labrax*, in waters around England and Wales. *Journal of the Marine Biological Association of the United Kingdom*, *76*(1), 107–125. https://doi.org/10.1017/S0025315400029040

Pawson, M. G., Pickett, G. D., Leballeur, J., Brown, M., & Fritsch, M. (2007). Migrations, fishery interactions, and management units of sea bass (*Dicentrarchus labrax*) in Northwest Europe. *ICES Journal of Marine Science*, *64*, 332–345. https://doi.org/10.1093/icesjms/fsl035

Petitgas, P. (1998). Biomass-dependent dynamics of fish spatial distributions characterized by geostatistical aggregation curves. *ICES Journal of Marine Science*, *55*(3), 443–453. https://doi.org/10.1006/jmsc.1997.0345

Petitgas, P., Reid, D., Planque, B., Nogueira, E., O'Hea, B., & Cotano, U. (2006). *The entrainment hypothesis: an explanation for the persistence and innovation in spawning migrations and life cycle spatial patterns*. ICES Document CM.

Petitgas, P., Woillez, M., Doray, M., & Rivoirard, J. (2016). A geostatistical definition of hotspots for fish spatial distributions. *Mathematical Geosciences*, *48*(1), 65–77. https://doi.org/10.1007/s11004-015-9592-z

Pickett, G. D., & Pawson, M. G. (1994). *Seabass: biology, exploitation, and conservation*, 1st ed. London; New York: Chapman & Hall.

Planque, B., Loots, C., Petitgas, P., Lindstrøm, U. L. F., & Vaz, S. (2011). Understanding what controls the spatial distribution of fish populations using a multi-model approach. *Fisheries Oceanography*, *20*(1), 1–17. https://doi.org/10.1111/j.1365-2419.2010.00546.x

Rue, H., Martino, S., & Chopin, N. (2009). Approximate Bayesian inference for latent Gaussian models by using integrated nested Laplace approximations. *Journal of the Royal Statistical Society: Series B (statistical methodology)*, *71*(2), 319–392. https://doi.org/10.1111/j.1467-9868.2008.00700.x

Rue, H., Martino, S., Lindgren, F., Simpson, D., Riebler, A., & Krainski, E. T. (2014). *INLA: Functions which allow to perform full Bayesian analysis of latent Gaussian models using Integrated Nested Laplace Approximaxion*. R package version 0.0-1404466487. R-INLA. http://www.R-INLA.org

SHOM (2015). *MNT Bathymétrique de façade Atlantique*. SHOM (Projet Homonim).

Thompson, B. M., & Harrop, R. T. (1987). The distribution and abundance of bass (*Dicentrarchus labrax*) eggs and larvae in the English Channel and southern North Sea. *Journal of the Marine Biological Association of the United Kingdom*, *67*(2), 263–274. https://doi.org/10.1017/S0025315400026588

Vázquez, F. J. S., & J. A. Muñoz-Cueto (Eds.) (2014). *Biology of European sea bass*. CRC Press.

Vinagre, C., Ferreira, T., Matos, L., Costa, M. J., & Cabral, H. N. (2009). Latitudinal gradients in growth and spawning of sea bass, *Dicentrarchus labrax*, and their relationship with temperature and photoperiod. *Estuarine, Coastal and Shelf Science*, *81*(3), 375–380. https://doi.org/10.1016/j.ecss.2008.11.015

Woillez, M., Fablet, R., Ngo, T. T., Lalire, M., Lazure, P., & De Pontual, H. (2016). A HMM-based model to geolocate pelagic fish from high-resolution individual temperature and depth histories: European sea bass as a case study. *Ecological Modelling*, *321*, 10–22. https://doi.org/10.1016/j.ecolmodel.2015.10.024

Woillez, M., Poulard, J. C., Rivoirard, J., Petitgas, P., & Bez, N. (2007). Indices for capturing spatial patterns and their evolution in time, with application to European hake (*Merluccius merluccius*) in the Bay of Biscay. *ICES Journal of Marine Science*, *64*(3), 537–550. https://doi.org/10.1093/icesjms/fsm025

## SUPPORTING INFORMATION

Additional supporting information may be found online in the Supporting Information section.

**How to cite this article:** Dambrine C, Woillez M, Huret M, de Pontual H. Characterising Essential Fish Habitat using spatio-temporal analysis of fishery data: A case study of the European seabass spawning areas. *Fish Oceanogr.* 2021;30:413–428. https://doi.org/10.1111/fog.12527